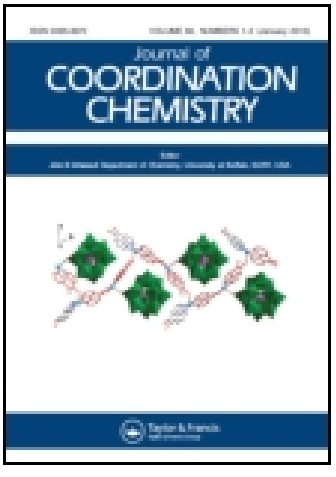

Journal of Coordination Chemistry
Publication details, including instructions for authors and subscription information:
http://www.tandfonline.com/loi/gcoo20

Solvent-dependent formation of two Pb(II) coordination polymers based on 4,4′-azodibenzoic acid linker: crystal structures, fluorescence, and thermal properties

Lei-Lei Liu[a], Ji-Min Du[a], Yuan-Ying Liu[a], Feng Zhao[a] & Feng-Ji Ma[a]
[a] College of Chemistry and Chemical Engineering, Anyang Normal University, Anyang, PR China
Accepted author version posted online: 10 Jan 2014.Published online: 22 Jan 2014.

To cite this article: Lei-Lei Liu, Ji-Min Du, Yuan-Ying Liu, Feng Zhao & Feng-Ji Ma (2014) Solvent-dependent formation of two Pb(II) coordination polymers based on 4,4′-azodibenzoic acid linker: crystal structures, fluorescence, and thermal properties, Journal of Coordination Chemistry, 67:1, 136-148, DOI: 10.1080/00958972.2013.878025

To link to this article: http://dx.doi.org/10.1080/00958972.2013.878025

Journal of Coordination Chemistry, 2014
Vol. 67, No. 1, 136–148, http://dx.doi.org/10.1080/00958972.2013.878025

Solvent-dependent formation of two Pb(II) coordination polymers based on 4,4′-azodibenzoic acid linker: crystal structures, fluorescence, and thermal properties

LEI-LEI LIU*, JI-MIN DU, YUAN-YING LIU, FENG ZHAO and FENG-JI MA

College of Chemistry and Chemical Engineering, Anyang Normal University, Anyang, PR China

(*Received 4 April 2013; accepted 5 November 2013*)

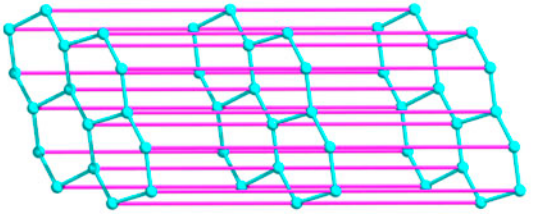

Solvothermal reactions of $Pb(OAc)_2{\cdot}2H_2O$ with 4,4′-azodibenzoic acid (H_2L) in DMSO (DMSO = dimethyl sulfoxide) and DMF/H_2O (DMF = N,N′-dimethylformamide) at 90 °C gave two Pb(II) coordination polymers (CPs), $[PbL(DMSO)]_n$ (**1**) and $[PbL(H_2O)]_n$ (**2**). Complexes **1** and **2** were characterized by elemental analysis, IR spectroscopy, powder X-ray diffraction, and single-crystal X-ray diffraction. Compound **1** possesses a 2-D staircase-like network based on pairs of left and right helical 1-D $[Pb(CO_2)_2(DMSO)]_n$ chains, and is further assembled into a 3-D supramolecular architecture with a $4^{12}6^3$ topology through intermolecular hydrogen bond interactions between the neighboring networks. Within the 1-D Pb–O–Pb chain, the DMSO terminally coordinates to Pb(II). Complex **2** has a 3-D motif containing 2-D Pb-carboxylate layers with H_2O bridging neighboring Pb ions in a 4^66^4 topological structure. The formation of **1** and **2** provides insight into the effect of solvents on the construction of CPs under solvothermal conditions. Stabilities and photoluminescent properties of **1** and **2** were also investigated.

Keywords: Lead(II) complex; 4,4′-Azodibenzoic acid; Crystal structure; Thermal stability; Luminescent property

1. Introduction

Coordination polymers (CPs) have been widely investigated because of their intriguing topologies, crystal packing motifs [1], and potential applications in gas storage and adsorption [2], catalysis [3], separation [4], and drug delivery [5]. Crystal engineering affords a powerful tool for design of coordination frameworks [6]. The ultimate aim is to control the higher structures of the target products and to investigate the relationship

*Corresponding author. Email: liuleileimail@163.com

between structure and properties. Thus, design and synthesis of CPs with desired properties has been a long-term challenge. Many factors such as coordination modes of the metal ions, metal/ligand ratios, ligands, pH, solvent, and temperature can affect the resulting architectures of the complexes [7, 8]. Minor changes of these synthetic factors may lead to different architectures originating from differences in connectivity or network catenation [9]. As an important factor, solvent often directly or indirectly influences the coordination behavior of the metal ions, as it can participate in coordination or influence the overall frameworks without participating in coordination [10]. Li *et al.* reported the solvent-controlled synthesis of three Cd(II) CPs based on a C_2-symmetric tricarboxylate linker [11].

Azobenzenecarboxylates, such as azobenzene-dicarboxylic, azobenzene-tricarboxylic, and azobenzene-tetracarboxylic acids, represent a type of bridging aromatic carboxylate utilized to construct functional CPs [12]. For example, Lu and co-workers reported three porous metal-organic frameworks (MOFs) using azobenzene-3,5,4′-tricarboxylic acid and $Cd(NO_3)_2{\cdot}4H_2O/MnCl_2{\cdot}4H_2O$ as building blocks [13]. Qiu *et al.* used 3,3′,5,5′-azobenzene-tetracarboxylic acid as a building block to construct three 3-D microporous MOFs with NbO and PtS topologies, and having hydrogen storage and luminescent properties [14]. Baul and co-workers reacted mixed arylazobenzoic acids with organotin salts, producing a series of mono, di-, tri-, and tetra-organotin(II/IV) carboxylate compounds, which showed various supramolecular architectures [15]. Furthermore, these organotin complexes were extensively studied and screened *in vitro* and *in vivo* for antitumor and cytostatic activities [15, 16]. Yaghi used 4,4′-azodibenzoic acid (H_2L) to react with $Tb(NO_3)_3{\cdot}5H_2O$ to get an interpenetrating network of $\{Tb_2L_3[(CH_3)_2SO]_4{\cdot}16[(CH_3)_2SO]\}_n$ with large free volume [17]. Recently, You *et al.* reported a series of 3-D interpenetrating lanthanide(III) porous CPs based on $Ln(NO_3)_3{\cdot}6H_2O$ and H_2L which displayed paramagnetic properties [18]. Subsequently, N-containing ligands such as pyridine [19], 1,10-phenanthroline [19], 4,4′-bipyridine [20], (4-pyridyl)ethylene [21], isonicotinate [22], 1,2-bis(imidazol-1-ylmethyl)benzene [23], and 1,4-bis(2-methyl-imidazol-1-yl)butane [24] were introduced into H_2L-based systems, and further assembled with Zn^{2+}, Cd^{2+}, Co^{2+}, and In^{3+} to give diverse CPs, which exhibited various topologies as well as adsorption and photoluminescence properties. Studies engaged in the assembly of 4,4′-azodibenzoic acid with Pb(II) have not been reported. As lead has a large ionic radius and high and variable coordination numbers, it has been widely employed to construct complicated CPs. In this work, solvothermal reactions of $Pb(OAc)_2{\cdot}2H_2O$ with 4,4′-azodibenzoic acid (H_2L) in DMSO and DMF/H_2O at 90 °C gave two Pb(II) CPs, $[PbL(DMSO)]_n$ (**1**) and $[PbL(H_2O)]_n$ (**2**). The results indicated that the solvent significantly affected the formation of lead(II) CPs. Here we describe the solvent-oriented reactions along with the crystal structures, thermal stabilities, and photoluminescent properties of **1** and **2**.

2. Experimental

2.1. *Materials and general methods*

H_2L was prepared according to literature methods [25]. All chemicals and reagents were obtained from commercial sources and used as received. IR spectra were recorded as KBr pellets on a Varian 800 FT-IR spectrometer from 4000 to 400 cm^{-1}. The C, H, and N elemental analyses were performed on an EA1110 CHNS elemental analyzer. Powder X-ray diffraction (PXRD) measurements were performed on a Bruker Ultima III X-ray diffractometer with Cu Kα ($\lambda = 1.5418$ Å) radiation. Luminescence spectra were recorded with a

Rigaku RIX 2000 fluorescence spectrophotometer. Thermal analyses were performed with a Netzsch STA-409 PC thermogravimetric (TG) analyzer at a heating rate of 10 °C min^{-1} and a flow rate of 100 cm^3 min^{-1} (N_2).

2.2. *Synthesis of 1 and 2*

2.2.1. [PbL(DMSO)]$_n$ (1). A mixture of $Pb(OAc)_2 \cdot 2H_2O$ (19 mg, 005 mM), H_2L (7 mg, 0.025 mM), and DMSO (4 mL) was sealed in a 10-mL Pyrex glass tube, heated at 120 °C for four days, and then cooled to room temperature at 5 °C/h. Red, block-shaped crystals of **1** (12 mg, 87% yield based on H_2L) were collected and washed thoroughly with DMSO and dried in air. Anal. Calcd for $C_{16}H_{14}N_2SPbO_5$: C, 37.72; H, 2.55; N, 5.06. Found: C, 37.57; H, 2.39; N, 5.21. IR (KBr disk): 3371 (m), 3071 (w), 1588 (s), 1511 (s), 1388 (m), 1363 (m), 1307 (m), 1218 (m), 1160 (w), 1132 (m), 1097 (m), 1010 (m), 878 (m), 860 (w), 798 (m), 706 (w), 629 (w), 500 (w) cm^{-1}.

2.2.2. [PbL(H_2O)]$_n$ (2). Compound **2** was prepared in the same way as **1**, except using DMF/H_2O (4 mL, 1 : 1 v/v) instead of DMSO The orange flakes of **2** (10 mg, 81% yield based on H_2L) were collected and washed thoroughly with DMF and dried in air. Anal. Calcd for $C_{14}H_{10}N_2PbO_5$: C, 34.08; H, 2.04; N, 5.68. Found: C, 34.15; H, 1.99; N, 5.45. IR (KBr disk): 3234 (m), 3058 (w), 1588 (s), 1509 (s), 1386 (m), 1362 (m), 1307 (m),

Table 1. Summary of crystallographic data and refinement parameters for **1** and **2**.

Compound	**1**	**2**
Empirical formula	$C_{16}H_{14}N_2O_5PbS$	$C_{14}H_{10}N_2O_5Pb$
Formula weight	553.56	493.44
Crystal system	Monoclinic	Monoclinic
Space group	$P2_1/c$	$C2/c$
a (Å)	13.359(3)	32.613(7)
b (Å)	7.6450(15)	7.3748(15)
c (Å)	17.209(3)	11.306(2)
β (°)	94.33(3)	105.71(3)
V (Å^3)	1752.5(6)	2617.7(10)
Z	4	8
ρ_{Calcd} (g/cm^3)	2.098	2.504
F (000)	1048.0	1840.0
μ (Mo Kα, mm^{-1})	9.775	12.918
Total reflections	11797	7132
Unique reflections	3085	2301
No. of observations	2756	1753
No. of parameters	228	199
R_1[a], wR_2[b] [$I > 2\sigma(I)$]	0.0199/0.0476	0.0557/0.1333
R_1[a], wR_2[b] (all data)	0.0238/0.0495	0.0917/0.1545
GOF[c]	1.025	1.065
$\Delta\rho_{min}/\Delta\rho_{max}$/e·Å^{-3}	0.762/−0.934	5.802/−3.181

[a] $R_1 = \Sigma||F_o|-|F_c||/\Sigma|F_o|$.
[b] $wR_2 = \{\Sigma w(F_o^2-F_c^2)^2/\Sigma w(F_o^2)^2\}^{1/2}$.
[c] $GOF = \{\Sigma w(F_o^2-F_c^2)^2/(n-p)\}^{1/2}$.
where n = number of reflections and p = total numbers of parameters refined.

1217 (m), 1160 (w), 1135 (m), 1096 (w), 1008 (m), 860 (m), 805 (w), 784 (m), 692 (w), 627 (w), 497 (w) cm^{-1}.

2.3. *X-ray crystallographic studies*

Single crystals of **1** and **2** were obtained directly from the above preparations. The crystals were mounted on glass fibers. All measurements were made at 296 K on a Bruker Smart Apex-II CCD area detector using graphite-monochromated Mo Kα ($\lambda = 0.071073$ nm) radiation. Diffraction data were collected at f and ω modes with a detector distance of 35 mm to the crystals. Cell parameters were refined by using Bruker *SAINT*. The collected data were reduced using *SAINT* and multi-scan absorption corrections were applied. The reflection data were also corrected for Lorentz and polarization effects.

The crystal structures were solved by direct methods refined on F^2 by full-matrix least squares with SHELXTL-97 [26]. In **2**, hydrogens of coordinated water (O1 *W*) were located from difference Fourier maps and refined with geometric restraints [O–H = 0.85(2) Å]. All other hydrogens in **1** and **2** were placed in geometrically idealized positions and constrained to ride on their parent. A summary of the key crystallographic data and refinement parameters for **1** and **2** is tabulated in table 1, and selected bond distances and angles are given in table 2.

Table 2. Selected bond distances (Å) and angles (°) for **1** and **2**[a].

Complex **1**			
Pb(1)−O(1)	2.779(3)	Pb(1)−O(2)	2.368(2)
Pb(1)−O(3A)	2.560(3)	Pb(1)−O(4A)	2.444(3)
Pb(1)−O(1C)	2.888(3)	Pb(1)−O(3B)	2.851(3)
Pb(1)−O(5)	2.442(3)	N(1)−N(2)	1.247(5)
O(2)−Pb(1)−O(5)	81.98(9)	O(4A)−Pb(1)−O(3A)	51.78(9)
O(2)−Pb(1)−O(4A)	94.95(10)	O(5)−Pb(1)−O(4A)	79.11(9)
O(2)−Pb(1)−O(3A)	98.21(11)	O(5)−Pb(1)−O(3A)	130.84(9)
O(4A)−Pb(1)−O(3A)	51.78(9)	O(2)−Pb(1)−C(14A)	100.36(10)
O(5)−Pb(1)−C(14A)	104.93(9)	O(4A)−Pb(1)−C(14A)	25.90(9)
O(3A)−Pb(1)−C(14A)	26.22(9)	N(1)−N(2)−C(8)	113.6(3)
N(2)−N(1)−C(5)	114.5(3)		
Complex **2**			
Pb(1)−O(1)	2.458(12)	Pb(1)−O(2)	2.559(10)
Pb(1)−O(1E)	2.777(8)	Pb(1)−O(2C)	2.874(6)
Pb(1)−O(3)	2.494(8)	Pb(1)−O(3D)	2.662(8)
Pb(1)−O(1W)	2.700(7)	Pb(1)−O(1WC)	2.601(8)
N(1)−N(1C)	1.23(2)	N(2)−N(2D)	1.23(2)
O(1)−Pb(1)−O(3)	86.2(3)	O(1)−Pb(1)−O(2)	51.3(3)
O(3)−Pb(1)−O(2)	75.6(3)	O(1)−Pb(1)−O(1WA)	76.4(3)
O(3)−Pb(1)−O(1WA)	67.7(3)	O(2)−Pb(1)−O(1WA)	117.1(3)
O(1)−Pb(1)−O(3B)	01.7(3)	O(3)−Pb(1)−O(3B)	136.0(2)
O(2)−Pb(1)−O(3B)	76.4(3)	O(1 WA)−Pb(1)−O(3B)	156.4(2)
O(1)−Pb(1)−O(1W)	118.3(3)	O(3)−Pb(1)−O(1W)	74.2(3)
O(2)−Pb(1)−O(1W)	67.2(3)	O(1WA)−Pb(1)−O(1W)	138.0(2)
O(3B)−Pb(1)−O(1W)	63.9(2)	O(1WA)−Pb(1)−C(1)	94.6(3)
O(1)−Pb(1)−C(1)	25.5(3)	O(3)−Pb(1)−C(1)	76.5(3)
O(2)−Pb(1)−C(1)	26.2(3)	O(3B)−Pb(1)−C(1)	92.2(3)
O(1W)−Pb(1)−C(1)	92.8(3)	Pb(1B)−O(1W)−Pb(1)	98.0(2)
N(1C)−N(1)−C(5)	115.2(14)	N(2D)−N(2)−C(12)	113.9(17)

[a]Symmetry codes for **1**: A: $x+1$, $-y+3/2$, $z+1/2$; B: $-x+1$, $-y+1$, $-z+1$; C: $-x+2$, $y-1/2$, $-z+3/2$; for **2**: A: $-x+1$, y, $-z+3/2$; B: $-x+1$, $-y$, $-z+1$; C: $-x+1/2$, $y-1/2$, $-z+1/2$; D: $-x+1/2$, $y+1/2$, $-z+1/2$; E: $-x+1/2$, $-y+1/2$, $-z+1$.

3. Results and discussion

3.1. *Synthesis consideration and general characterization*

Reactions of $Pb(OAc)_2{\cdot}2H_2O$ with H_2L with molar ratio of $Pb(OAc)_2{\cdot}2H_2O$ to H_2L 2 : 1 in DMSO for four days at 120 °C and cooled to ambient temperature at a rate of 5 °C/h produced red crystals of **1** (87% yield). An analogous reaction, except using DMF/H_2O (4 mL, 1 : 1, v/v) instead of DMSO, afforded orange crystals of **2** (81% yield). As described later in this article, the solvents influence the coordination architectures of **1** and **2** via directly coordinating to Pb(II) as a terminal ligand in **1** (DMSO) and a bridging linker in **2** (H_2O). DMF did not coordinate to Pb in **2**, which may be due to stronger coordination bonds between Pb^{2+} and H_2O than between Pb^{2+} and DMF. When pure DMF was used instead of a mixed DMF/H_2O solvent, no crystals were produced. The polarity of H_2O is higher than that of DMSO and DMF, as well as the latter having a larger steric hindrance, which may also lead to water as a bridging linker, resulting in the 3-D MOF of **2**. In analogous reactions at 90 °C, **1** and **2** were obtained in lower yields (80% for **1** and 57% for **2**). We also attempted crystallization in other solvents, such as H_2O, DMSO/DMF, and DMSO/H_2O, but without success. When the reaction temperature fell to 70 °C, only orange precipitates were isolated, and their PXRD patterns were inconsistent with those of **1** and **2**.

Due to good antitumor and cytostatic properties of Sn complexes, similar experiments to synthesize the Sn derivatives of **1** and **2** were performed. Reactions of $SnCl_4$ with H_2L in DMSO or DMF/H_2O at 90 °C provided a white precipitate and an orange solution. The IR spectrum and PXRD pattern suggested that the white precipitate was SnO_2, and ^1H NMR spectroscopy identified H_2L as a component of the orange solution (figure S1, see online supplemental material at http://dx.doi.org/10.1080/00958972.2013.878025). These results indicate that $SnCl_4$ was easily hydrolyzed under solvothermal conditions. Mixing $SnCl_4$ and H_2L in DMSO or DMF/H_2O at room temperature and stirring for 1 h produced an orange solution. After standing for one week, an orange precipitate was generated, which was also identified as H_2L by ^1H NMR spectroscopy. Organotin compounds Me_2SnO and Ph_2SnO reacted with H_2L to give red precipitates. The PXRD patterns were inconsistent with those of Pb-based complexes **1** and **2**. Crystallization from other solvents, such as DMSO and DMSO/DMF, always failed to form any crystals.

Compounds **1** and **2** were stable towards oxygen and moisture, and almost insoluble in common organic solvents, such as $CHCl_3$, MeOH, MeCN, and DMF. The IR spectra of **1** and **2** show peaks at 1588–1590 cm^{-1} and 1386–1388 cm^{-1}, indicative of the existence of coordinated carboxylic groups [27]. Peaks at 1509–1511 cm^{-1} are assigned to the asymmetric N=N vibrations of **1** and **2** [7f]. The identities of **1** and **2** were further confirmed by single-crystal diffraction analysis.

3.2. *Description of the crystal structures*

3.2.1. $[PbL(DMSO)]_n$ (1). Compound **1** crystallized in the monoclinic space group $P2_1/c$ and its asymmetric unit contains one [PbL(DMSO)] As shown in figure 1(a), each Pb in **1** is seven-coordinate by O1, O2, O3, and O4A from the chelating carboxylates of two L^{2-}, O3B and O1C, from two bridging carboxylates of two different L^{2-}, and O5 from a terminal DMSO. The two carboxylates of L^{2-} in **1** both adopt chelating/bridging (μ_2–$\eta^2:\eta^1$) coordination. Comparing the two groups, the average chelating Pb–O and bridging Pb–O bond distances (O1, O2, 2.573(5) Å *versus* O1C, 2.888(3) Å, respectively) in one carboxylate

are a little longer than those in the other carboxylate [O3A, O4A, 2.502(5) Å *versus* O3B, 2.851(3) Å, respectively; figure 1(a) and table 2]. The DMSO Pb–O bond length (2.442(3) Å) is shorter than that in $[Pb(p\text{-BDC})(DMSO)]_n$ (2.595(5) Å, *p*-BDC = 1,4-benzenedicarboxylate) [28]. Each $[Pb(CO_2)(DMSO)]^+$ unit in **1** is interlinked by another carboxylate to form a 1-D helical $[Pb(CO_2)_2(DMSO)]_n$ chain extending along the *b* axis [figure 1(b)]. Within the 1-D chain, neighboring Pb···Pb separation is 4.448(5) Å and the Pb···Pb···Pb angle is 118.4°,

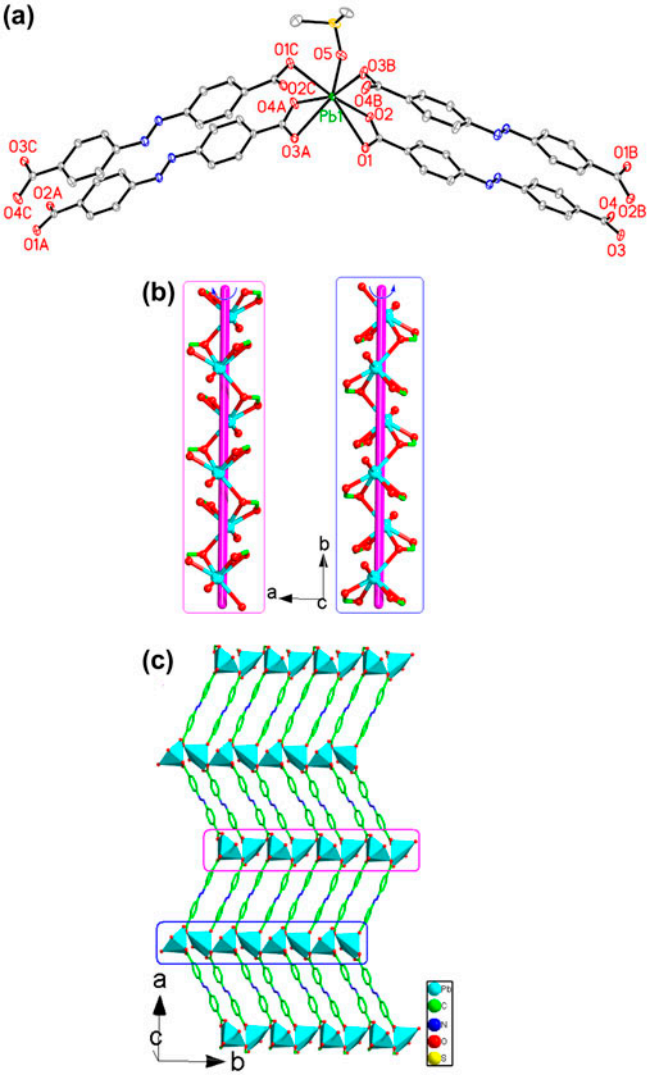

Figure 1. (a) View of the coordination environment of Pb in **1** with atom-labeling scheme and 25% probability ellipsoids. Symmetry codes: (A) $x+1, -y+3/2, z+1/2$; (B) $-x+1, -y+1, -z+1$; (C) $-x+2, y-1/2, -z+3/2$. (b) View of the 1-D $[Pb(CO_2)_2(DMSO)]_n$ left- and right-handed helical chains in **1** extending along the *b* axis. (c) View of a 2-D staircase-like network in **1** extending along the *ab* plane. (d) View of a 3-D hydrogen-bonded architecture in **1** along the *b* axis. (e) Schematic view of a $4^{12}6^3$ topological net of **1**. All hydrogens except those related to H-bonding interactions and coordinated DMSO are omitted for clarity.

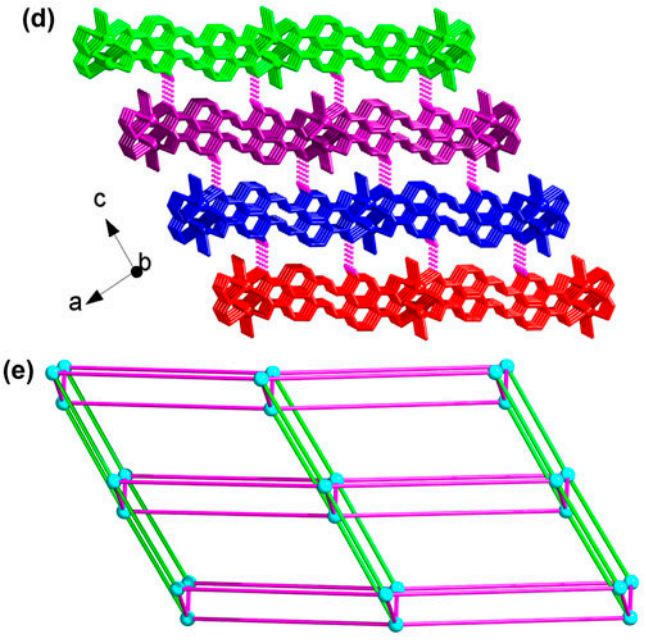

Figure 1. (*Continued*)

comparable with analogous lead(II) polymers [29]. These adjacent 1-D Pb–O–Pb chains are bridged by L^{2-} to form a 2-D staircase-like network with parallelogram-shaped meshes (4.45 × 17.56 Å^2) extending along the *ab* plane [figure 1(c)]. Adjacent 1-D Pb–O–Pb chains are left- and right-handed helices [figure 1(b)], which has been observed in previously reported Pb(II) complexes [30]. O4 of the carboxylate forms an intermolecular hydrogen bond with H6 of a phenyl in the adjacent 2-D network (C6–H6···O4, 3.328(5) Å). These hydrogen-bonding interactions hold the 2-D networks together to generate a 3-D hydrogen-bonded architecture extending along the *ac* plane [figure 1(d)]. Topologically [31], if the Pb(II) centers are considered as nodes and the L^{2-} and hydrogen bonds are considered as linkers, the structure of **1** can be specified by the Schläfli symbol $4^{12}6^3$ [figure 1(e)]. The Yaghi and You groups reported the frameworks $[Tb_2L_3(DMSO)_4{\cdot}16DMSO]_n$, $[Ln_2L_3(DMSO)_4{\cdot}6DMSO{\cdot}8H_2O]_n$ (Ln = Ce, Sm, Eu, Gd) and $\{[Ce_3L_3(HL)_3]{\cdot}30DMSO{\cdot}29H_2O\}_n$ based on the assembly of H_2L with $Ln(NO_3)_3{\cdot}6H_2O$ in DMSO [17, 18]. The Ln centers in these complexes are bridged by carboxylates of L^{2-} to form dinuclear $[Tb_2(CO_2)_6]$ and $[Ln_2(CO_2)_4]$ units, as well as trinuclear $[Ce_3(CO_2)_6]$ units, different from the Pb(II) in **1**, which are bridged by carboxylates of L^{2-} ligands to generate infinite helical $[Pb(CO_2)_2(DMSO)]_n$ chains. Furthermore, the dinuclear or trinuclear units in these Ln-based CPs act as six-connecting nodes, linking equivalent units via sharing L^{2-} ligands to form 3-D interpenetrating structures. However, **1** possesses a 2-D staircase-like network based on pairs of 1-D left and right helical $[Pb(CO_2)_2(DMSO)]_n$ chains and further assembled into a 3-D supramolecular architecture through intermolecular hydrogen bond interactions. These differences may be ascribed to the different metal centers in these polymers.

3.2.2. $[PbL(H_2O)]_n$ (2). Compound **2** crystallizes in the monoclinic space group *C2/c* and its asymmetric unit contains one $[PbL(H_2O)]$ The coordination environment of Pb^{2+} in **2** is different from that in **1**. Each Pb in **2** is eight-coordinate by O3, O3D, O2C, and O1E of four bridging carboxylates from four L^{2-}, O1 and O2 of one chelating carboxylate from a fifth L^{2-}, as well as O1W and O1WC from two bridging waters [figure 2(a)]. The two carboxylate groups of L^{2-} in **2** adopt chelating-bridging (μ_2–$\eta^2:\eta^2$) [O1, O2, green moiety in figure 2(d)] and bridging (μ_2–$\eta^1:\eta^1$) [O3, O3D, pink moiety in figure 2(d)] coordination. For the chelating-bridging carboxylates in **2**, both the average chelation Pb–O (O1, O2, 2.509(5) Å) and the bridging Pb–O bond lengths [O1E, O2C, 2.825(5) Å; figure 2(a) and

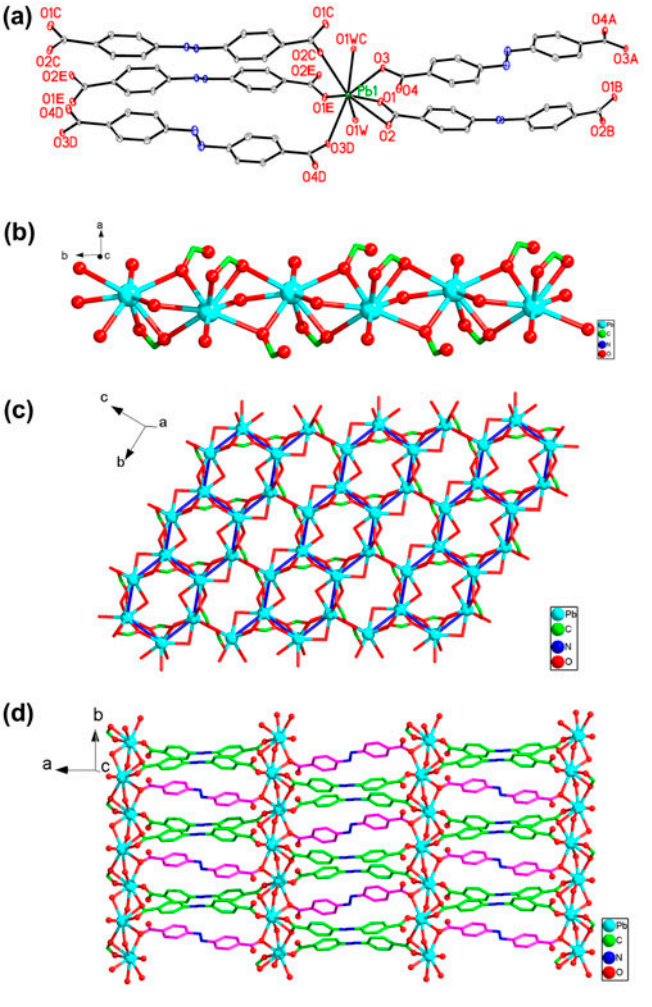

Figure 2. (a) View of the coordination environment of Pb in **2** with atom-labeling scheme and 25% probability ellipsoids. Symmetry codes: (A) $-x+1$, y, $-z+3/2$; (B) $-x+1$, $-y$, $-z+1$; (C) $-x+1/2$, $y-1/2$, $-z+1/2$; (D) $-x+1/2$, $y+1/2$, $-z+1/2$; (E) $-x+1/2$, $-y+1/2$, $-z+1$. (b) View of a 1-D $[Pb(CO_2)_2(H_2O)]_n$ chain in **2** extending along the *b* axis. (c) View of a 2-D Pb–carboxylate layer in **2** extending along the *bc* plane. (d) View of a 2-D network in **2** extending along the a*b* plane. Atom color codes: Pb, cyan; O, red; N, blue; and C, green or pink. (e) View of the 3-D motif in **2** along the *b* axis. (f) Schematic view of a 4^66^4 topological net of **2**. All hydrogens are omitted for clarity. (see http://dx.doi.org/10.1080/00958972.2013.878025 for color version)

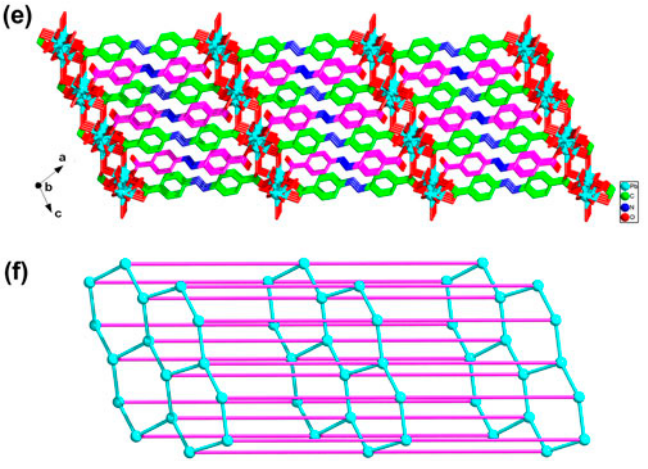

Figure 2. (*Continued*).

table 2] are a little shorter than analogous distances in **1** (averages, 2.537(5) and 2.869(3) Å, respectively). For the bridging carboxylate in **2**, the mean bridging Pb–O bond distance [O3 and O3D, 2.577(5) Å; figure 2(a) and table 2] is shorter than that observed in [NaPb(1,3,5-BTC)$(H_2O)]_n$ (2.753(6) Å, 1,3,5-BTC = 1,3,5-benzenetricarboxylate) [32(a)]. The average water Pb–O bond distance (2.650(7) Å) is shorter than that in the related structure [Pb(proline)$(H_2O)]_n$ (2.733(5) Å) [32(b)]. The mean N=N (1.230(2) Å) bond length in **2** is slightly shorter than that in **1** (1.247(5) Å). Each $[Pb(CO_2)]^+$ unit in **2** is bridged by another carboxylate and H_2O molecules to form a 1-D $[Pb(CO_2)_2(H_2O)]_n$ chain extending along the *b* axis [figure 2(b)]. Compared with the 1-D helical chain of **1**, Pb ions in **2** are bridged not only by the chelating/bridging carboxylates but also bridging carboxylates and H_2O, without the formation of a helical axis. Furthermore, adjacent 1-D $[Pb(CO_2)_2(H_2O)]_n$ chains in **2** are interlinked via shared carboxylates to afford a 2-D Pb–carboxylate layer extending along the *bc* plane [figure 2(c)]. In the 2-D layer of **2**, the neighboring six Pb ions are bridged by H_2O and carboxylate producing a benzene-like six Pb unit [blue lines in figure 2(c)]. In this unit, the Pb···Pb separations are 4.000(1) and 4.296(6) Å, and the Pb···Pb···Pb angles within the Pb_4O_8 node are 113.2°, 104.9°, and 134.4°, which are similar with those of the Pb–O–Pb chains of **1**. The 1-D $[Pb(CO_2)_2(H_2O)]_n$ chains of **2** are linked via L^{2-} to give a 2-D network extending along the *ab* plane [figure 2(d)]. Furthermore, each 2-D Pb–carboxylate layer is bridged by L^{2-} to afford a 3-D structure [figure 2(e)] extending along the *ac* plane. From a topological point of view, such a 3-D motif can be simplified into a 4^66^4 topological net [figure 2(f)]. The reported Zn/Cd/Al-based polymers, $[ZnL(H_2O)]_n$, $[CdL_2{\cdot}H_2O]_n$, $[CdL(H_2O)_2]_n$, and $[Al(\mu_2\text{-}OH)L]_n$, prepared by reactions of Zn(II)/Cd(II)/Al(III) salts with H_2L in H_2O or DMF/H_2O [12f, 12g, 19, 20], deserve comparison with **2**. The Zn/Cd/Al centers in their corresponding polymers showed five- or six-coordinate geometries and all reactions generated 1-D metal-carboxylate chains, which were further linked by L^{2-} to afford 1-D chains for $[CdL(H_2O)_2]_n$ and $[CdL_2{\cdot}H_2O]_n$ [19, 20], 2-D layers for $[Al(\mu_2\text{-}OH)L]_n$ [12g], and 3-D structure for $[ZnL(H_2O)]_n$ [12f]. However, **2** exhibits eight-coordinate geometry and forms 2-D Pb-carboxylate layers, thus affording a 3-D motif. The different structures between **2** and Zn/Cd/Al-based polymers may be due to the larger radius and higher coordination numbers for Pb than those of Zn/Cd/Al in the latter polymers.

The formation of different structures of **1** and **2** in different solvents deserves comment. The coordination numbers of Pb^{2+} in **1** and **2** are seven and eight, respectively, displaying disordered crowned triangular prismatic and dodecahedral geometries (figure 3). However, the arrangement of L and DMSO or H_2O around Pb(II) in both **1** and **2** do not show a gap or hole in the coordination geometry (holodirected geometry), indicating that the lone pair of electrons on lead(II) is inactive in these complexes [33]. The solvents in **1** and **2** have different functions, as a terminal molecule (DMSO) in **1** and as a bridging linker (H_2O) in **2**, which led to a 2-D network of **1** and the 3-D motif of **2**. So, solvent in this study greatly affected the coordination geometry of Pb and the overall structures of these compounds.

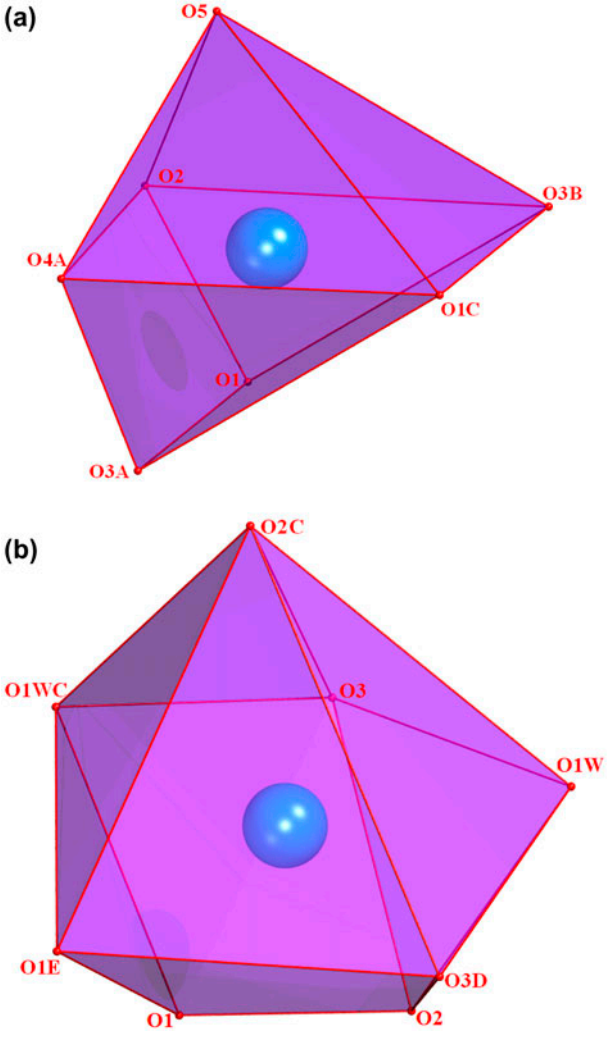

Figure 3. (a) PbO_7 polyhedron showing the coordination geometry of Pb in **1**. Symmetry codes: (A) $x+1, -y+3/2, z+1/2$; (B) $-x+1, -y+1, -z+1$; (C) $-x+2, y-1/2, -z+3/2$. (b) PbO_8 polyhedron showing the coordination geometry of Pb in **2**. Symmetry codes: (A) $-x+1, y, -z+3/2$; (B) $-x+1, -y, -z+1$; (C) $-x+1/2, y-1/2, -z+1/2$; (D) $-x+1/2, y+1/2, -z+1/2$; (E) $-x+1/2, -y+1/2, -z+1$.

3.3. *X-ray powder diffraction analyses and TG analyses*

Compounds **1** and **2** were also characterized by PXRD at room temperature. The patterns calculated from the single-crystal X-ray data of **1** and **2** were in agreement with the observed ones in almost identical peak positions (figure S2). The difference in reflection intensities between the simulated and experimental patterns is due to the powder size and variation in preferred orientation for the powder samples during collection of the experimental PXRD data.

TG analyses of **1** and **2** were carried out to study their thermal stabilities (figure S3). Both TG curves exhibit two distinct weight losses from 30 to 520 °C. The first weight loss of 12.06% for **1** at 165–246 °C is consistent with elimination of coordinated DMSO (Calcd: 14.11 wt.%). The second weight loss (37.19 wt.%) was observed at 410–525 °C, corresponding to decomposition of L^{2-} (Calcd: 37.61 wt.%). The remaining weight (40.68 wt.%) corresponds to that for PbO (40.32 wt.%), suggesting that this is the final product [34]. The TG curve of **2** indicates loss of coordination water of 3.21 wt.% (Calcd: 3.65 wt.%) from 140 to 198 °C. The second weight loss at 413–521 °C is attributed to the decomposition of the framework of **2**. The third weight loss (4.52 wt.%) at 725–775 °C may be ascribed to the loss of the azo groups (Calcd: 5.68 wt.%), perhaps present as lead nitride [27]. The final residue of 56.61 wt.% in **2** is in agreement with that for $PbCO_3$ (Calcd: 54.15 wt.%), as observed in previous studies [35]. In the DSC curves of **1** and **2** (figure S4), the endothermic events with maxima at 201 (**1**) and 180 °C (**2**) are attributed to the release of DMSO and H_2O, respectively [27]. Furthermore, the intense exothermic events with maxima at 496 (**1**) and 516 °C (**2**) suggest the decomposition of the organic framework of **1** and **2**. These results indicate that the frameworks of **1** and **2** are stable to 410 °C.

3.4. *Photoluminescent properties*

The photoluminescent properties of **1** and **2** in the solid state at room temperature were studied (figure S5). H_2L did not show photoluminescent properties. Excitation of **1** and **2** at 307 and 277 nm resulted in strong emission bands at 564 and 554 nm, respectively. The emissions for **1** and **2** may be assigned to metal-to-ligand charge transfer with electrons being transferred from Pb(II) to the unoccupied π^* orbitals of carboxylate [36], similar to other Pb-carboxylate-based polymers [37]. The shifts of emission bands occurring in **1** and **2** are probably due to cooperative effects of intra-ligand emission [38].

4. Conclusion

We synthesized, under solvothermal conditions, two solvent-directed Pb(II)-organic CPs based on a 4,4′-azodibenzoic acid linker. Compound **1** shows a 2-D staircase-like network based on pairs of 1-D left and right helical $[Pb(CO_2)_2(DMSO)]_n$ chains, and further assembled into a 3-D supramolecular architecture with a $4^{12}6^3$ topology through intermolecular hydrogen bond interactions between neighboring networks. Compound **2** has a 3-D motif based on 2-D Pb–carboxylate layers and exhibits a 4^66^4 topological structure. DMSO is terminally coordinated in **1,** and H_2O is a bridge in **2**. Carboxylates of L^{2-} adopt different coordination modes (bridging and bridging/chelating). Evidently, the solvent played an

important role in the formation of these Pb(II) CPs. This work highlights the delicate solvent-induced assembly in crystal engineering of functional CPs, which could lead to new compounds with interesting structures and properties.

Supplementary material

Figures of the ^{1}H NMR spectrum of the H_2L ligand; experimental and simulated PXRD patterns, TGA curves, DSC curves, emission spectra, and IR spectra for **1**−**2**. CCDC 911861 (**1**) and 911860 (**2**) contain the supplementary crystallographic data. These data can be obtained free of charge via www.ccdc.cam.ac.uk/data_request/cif (or from the Cambridge Crystallographic Data Center, 12 Union Road, Cambridge CB2 1EZ, UK; Fax: (44) 1223 336-033. E-mail: deposit@ccdc.cam.ac.uk).

Funding

This work was supported by the National Natural Science Foundation of China [U1304210, 21003001, 21273010, and 21105002]; the Projects of Ministry of Education of Returned Overseas Students [(2010) 1561]; and the Natural Science Projects of the Department of Education of Henan Province [13A150013].

References

[1] (a) F.A. Cotton, C. Lin, C. Murillo. *Acc. Chem. Res*., **34**, 759 (2001); (b) O.R. Evans, W.B. Lin. *Acc. Chem. Res*., **35**, 511 (2002); (c) G. Férey, C. Mellot-Draznieks, C. Serre, F. Millange. *Acc. Chem. Res*., **38**, 217 (2005); (d) J.P. Zhang, Y.B. Zhang, J.B. Lin, X.M. Chen. *Chem. Rev*., **112**, 1001 (2012); (e) W. Zhang, R.G. Xiong. *Chem. Rev*., **112**, 1163 (2012).

[2] (a) L.J. Murray, M. Dincă, J.R. Long. *Chem. Soc. Rev*., **38**, 1294 (2009); (b) J.R. Li, R.J. Kuppler, H.C. Zhou. *Chem. Soc. Rev*., **38**, 1477 (2009).

[3] (a) C.D. Wu, A. Hu, L. Zhang, W. Lin. *J. Am. Chem. Soc*., **127**, 8940 (2005); (b) J. Lee, O.K. Farha, J. Roberts, K.A. Scheidt, S.T. Nguyen, J.T. Hupp. *Chem. Soc. Rev*., **38**, 1450 (2009).

[4] V. Finsy, H. Verelst, L. Alaerts, D.E. De Vos, P.A. Jacobs, G.V. Baron, J.F.M. Denayer. *J. Am. Chem. Soc*, **130**, 7110 (2008).

[5] P. Horcajada, C. Serre, M. Vallet-Regi, M. Sebban, F. Taulelle, G. Férey. *Angew. Chem. Int. Ed*., **45**, 597 (2006).

[6] (a) B.F. Abrahams, P.A. Jackson, R. Robson. *Angew. Chem. Int. Ed*., **37**, 2656 (1998); (b) Y.F. Zhou, F.L. Jiang, D.Q. Yuan, B.L. Wu, R.H. Wang, Z.L. Lin, M.C. Hong. *Angew. Chem. Int. Ed*., **43**, 5665 (2004); (c) X.L. Zhao, H.Y. He, T.P. Hu, F.N. Dai, D.F. Sun. *Inorg. Chem*., **48**, 8057 (2009).

[7] (a) J.L. Du, T.L. Hu, J.R. Li, S.M. Zhang, X.H. Bu. *Eur. J. Inorg. Chem*., **2008,** 1059 (2008); (b) B. Xu, Z.J. Lin, L.W. Han, R.Cao. *CrystEngComm.*, **13**, 440 (2011). (c) J. Yang, G.D. Li, J.J. Cao, Q. Yue, G.H. Li, J.S. Chen. *Chem. –A. Eur. J*., **13**, 3248 (2007); (d) D. Sun, N. Zhang, R.B. Huang, L.S. Zheng. *Cryst. Growth Des*., **10**, 3699 (2010); (e) Y. Zhang, J. Yang, Y. Yang, J. Guo, J.F. Ma. *Cryst. Growth Des*., **12**, 4060 (2012); (f) L.L. Liu, Z.G. Ren, L.W. Zhu, H.F. Wang, W.Y. Yan, J.P. Lang. *Cryst. Growth Des*., **11**, 3479 (2011); (g) M.L. Tong, S. Kitagawa, H.C. Chang, M. Ohba. *Chem. Commun*., **40**, 418 (2004).

[8] (a) Y. Liu, Y. Qi, Y.H. Su, F.H. Zhao, Y.X. Che, J.M. Zheng. *CrystEngComm*., **12**, 3283 (2010); (b) P.M. Forster, N. Stock, A.K. Cheetham. *Angew. Chem. Int. Ed*., **44**, 7608 (2005); (c) B. Zheng, J.F. Bai, Z.X. Zhang. *CrystEngComm*., **12**, 49 (2010); (d) L.S. Long. *CrystEngComm.*, **12**, 1354 (2010); (e) J.S. Qin, D.Y. Du, S.L. Li, Y.Q. Lan, K.Z. Shao, Z.M. Su. *CrystEngComm*., **13**, 779 (2011); (f) H.X. Yang, S.Y. Gao, J. Lü, B. Xu, J.X. Lin, R. Cao. *Inorg. Chem*., **49**, 736 (2010); (g) H.J. Cheng, H.X. Li, Z.G. Ren, C.N. Lü, J. Shi, J.P. Lang. *CrystEngComm*., **14**, 6064 (2012); (h) P. Mahata, A. Sundaresan, S. Natarajan. *Chem. Commun*., 4471 (2007); (i) X.M. Lin, H.C. Fang, Z.Y. Zhou, L. Chen, J.W. Zhao, S.Z. Zhu, Y.P. Cai. *CrystEngComm*., **11**, 847 (2009).

[9] (a) J.J. Zhang, L. Wojtas, R.W. Larsen, M. Eddaoudi, M.J. Zaworotko. *J. Am. Chem. Soc*., **131**, 17040 (2009); (b) L.F. Ma, L.Y. Wang, D.H. Lu, S.R. Batten, J.G. Wang. *Cryst. Growth Des*., **9**, 1741 (2009); (c) S.M. Fang,

Q. Zhang, M. Hu, E.C. Sanudo, M. Du, C.S. Liu. *Inorg. Chem*., **49**, 9617 (2010); (d) L.L. Liu, L. Liu, J.J. Wang. *Inorg. Chim. Acta*, **397**, 75 (2013).
[10] (a) J.P. Lang, Q.F. Xu, R.X. Yuan, B.F. Abrahams. *Angew. Chem. Int. Ed*., **43**, 4741 (2004); (b) B.C. Tzeng, T.Y. Chang. *Cryst. Growth Des*., **9**, 5343 (2009); (c) S.C. Chen, R.R. Qin, Z.H. Zhang, J. Qin, H.B. Gao, F.A. Sun, M.Y. He, Q. Chen. *Inorg. Chim. Acta*, **390**, 61 (2012); (d) Y.Y. Liu, H.J. Li, Y. Han, X.F. Lv, H.W. Hou, Y.T. Fan. *Cryst. Growth Des*., **12**, 3505 (2012).
[11] L. Li, S.Y. Wang, T.L. Chen, Z.H. Sun, J.H. Luo, M.C. Hong. *Cryst. Growth Des*., **12**, 4109 (2012).
[12] (a) Y.Z. Tang, Y.H. Tan, J.W. Zhu, F.M. Ji, T.T. Xiong, W.Z. Xiao, C.F. Liao. *Cryst. Growth Des*., **8**, 1801 (2008); (b) A.J. Cairns, J.A. Perman, L. Wojtas, V.C. Kravtsov, M.H. Alkordi, M. Eddaoudi, M.J. Zaworotko. *J. Am. Chem. Soc*., **130**, 1560 (2008); (c) Y.G. Lee, H.R. Moon, Y.E. Cheon, M.P. Suh. *Angew. Chem. Int. Ed*., **47**, 7741 (2008); (d) W.L. Liu, L.H. Ye, X.F. Liu, L.M. Yuan, J.X. Jiang, C.G. Yan. *CrystEngComm.*, **10**, 1395 (2008); (e) W.B. Yu, Y.F. Han, Y.J. Lin, G.X. Jin. *Chem. –A. Eur. J*., **17**, 1863 (2011); (f) F. Fu, D.S. Li, X.G. Yang, C.Q. Zhang, Y.P. Wu, J. Zhao, E.B. Wang. *Inorg. Chem. Commun*., **12**, 657 (2009); (g) C. Volkringer, T. Loiseau, T. Devic, G. Férey, D. Popov, M. Burghammer, C. Riekel. *CrystEngComm.*, **12**, 3225 (2010).
[13] M. Meng, D.C. Zhong, T.B. Lu. *CrystEngComm.*, **13**, 6794 (2011).
[14] M. Xue, G.S. Zhu, Y.X. Li, X.J. Zhao, Z. Jin, E.H. Kang, S.L. Qiu. *Cryst. Growth Des.*, **8**, 2478 (2008).
[15] (a) T.S.B. Baul, W. Rynjah, X.Q. Song, G. Eng, A. Linden. *J. Organomet. Chem*., **692**, 3392 (2007); (b) T.S.B. Baul, K.S. Singh, A. Lyčka, A. Linden, X.Q. Song, A. Zapata, G. Eng. *Appl. Organomet. Chem*., **20**, 788 (2006); (c) T.S.B. Baul, W. Rynjah, E. Rivarola, A. Lyčka, M. Holčapek, R. Jirásko, D.D. Vos, R.J. Butcher, A. Linden. *J. Organomet. Chem*., **691**, 4850 (2006); (d) T.S.B. Baul, K.S. Singh, M. Holčapek, R. Jirásko, A. Linden, X.Q. Song, A. Zapata, G. Eng. *Appl. Organomet. Chem*., **19**, 935 (2005); (e) T.S.B. Baul, A. Paul, A. Linden. *J. Organomet. Chem*., **696**, 4229 (2012); (f) T.S.B. Baul, A. Paul, L. Pellerito, M. Scopelliti, C. Pellerito, P. Singh, P. Verma, A. Duthie, D.D. Vos, R.P. Verma, U. Englert. *J. Inorg. Biochem*., **104**, 950 (2010); (g) T.S.B. Baul, A. Paul, L. Pellerito, M. Scopelliti, A. Duthie, D.D. Vos, R.P. Verma, U. Englert. *J. Inorg. Biochem*., **107**, 119 (2012).
[16] (a) F.P. Pruchnik, M. Bańbuła, Z. Ciunik, M. Latocha, B. Skop, T. Wilczok. *Inorg. Chim. Acta*, **356**, 62 (2003); (b) S. Chakraborty, A.K. Bera, S. Bhattacharya, S. Ghosh, A.K. Pal, S. Ghosh, A. Banerjee. *J. Organomet. Chem*., **645**, 33 (2002); (c) A. Růžička, A. Lyčka, R. Jambor, P. Novák, I. Císařová, M. Holčapek, M. Erben, J. Holeček. *Appl. Organomet. Chem*., **17**, 168 (2003); (d) F.P. Pruchnik, M. Bańbula, Z. Ciunik, H. Chojnacki, M. Latocha, B. Skop, T. Wilczok. *Appl. Organomet. Chem*., **16**, 587 (2002); (e) F.P. Pruchnik, M. Bańbula, Z. Ciunik, H. Chojnacki, M. Latocha, B. Skop, T. Wilczok, A. Opolski, J. Wietrzyk, A. Nasulewicz. *Eur. J. Inorg. Chem*., **2002**, 3214 (2002).
[17] M.R. Theresa, E. Mohamed, M. David, M. O'Keeffe, O.M. Yaghi. *J. Am. Chem. Soc.*, **122**, 4843 (2000).
[18] Y.F. Han, X.Y. Li, L.Q. Li, C.L. Ma, Z. Shen, Y. Song, X.Z. You. *Inorg. Chem.*, **49**, 10781 (2010).
[19] Z.F. Chen, Z.L. Zhang, Y.H. Tan, Y.Z. Tang, H.K. Fun, Z.Y. Zhou, B.F. Abrahams. *CrystEngComm.*, **10**, 217 (2008).
[20] S. Bhattacharya, U. Sanyal, S. Natarajan. *Cryst. Growth Des.*, **11**, 735 (2011).
[21] B.L. Chen, S.Q. Ma, E.J. Hurtado, E.B. Lobkovsky, H.C. Zhou. *Inorg. Chem.*, **46**, 8490 (2007).
[22] X.J. Gu, Z.H. Lu, Q. Xu. *Chem. Commun.*, **46**, 7400 (2010).
[23] J. Yang, J.F. Ma, S.R. Batten, S.W. Ng, Y.Y. Liu. *CrystEngComm.*, **13**, 5296 (2011).
[24] Y.L. Liu, K.F. Yue, B.H. Shan, L.L. Xu, C.J. Wang, Y.Y. Wang. *Inorg. Chem. Commun.*, **17**, 30 (2012).
[25] E.B. Reid, E.C. Pritchett. *J. Org. Chem.*, **18**, 715 (1953).
[26] G.M. Sheldrick, *SHELXS-97 and SHELXL-97, Program for X-ray Crystal Structure Solution*, University of Göttingen, Germany (1997).
[27] L.L. Liu, L.M. Wan, Z.G. Ren, J.P. Lang. *Inorg. Chem. Commun.*, **14**, 1069 (2011).
[28] J.D. Lin, S.T. Wu, Z.H. Li, S.W. Du. *CrystEngComm.*, **12**, 4252 (2010).
[29] (a) F. Marandi, J. Sartaji, G. Bruno, H.A. Rudbari. *J. Coord. Chem*., **65**, 1872 (2012); (b) F. Marandi, C.K.H. Quah, H.K. Fun. *J. Coord. Chem*., **66**, 986 (2013).
[30] G. Han, Y.J. Mu, D.Q. Wu, Y.Y. Jia, H.W. Hou, Y.T. Fan. *J. Coord. Chem.*, **65**, 3570 (2012).
[31] A.F. Wells. *Three-Dimensional Nets and Polyhedra*, Wiley-Interscience, New York (1977).
[32] (a) L. Zhang, Z.J. Li, Q.P. Lin, Y.Y. Qin, J. Zhang, P.X. Yin, J.K. Cheng, Y.G. Yao. *Inorg. Chem*., **48**, 6517 (2007); (b) F. Marandi, N. Shahbakhsh, *J. Coord. Chem*., **60**, 2589 (2007).
[33] (a) S.J. Jenniefer, P.T. Muthiah, R. Priyadharshni. *J. Coord. Chem*., **65**, 4397 (2012); (b) J.Y. Hu, S.S. Li, J.A. Zhao, S.F. Chen, H.W. Hou, H.P. Zhao. *J. Coord. Chem*., **65**, 1258 (2012).
[34] B. Wu, Z.G. Ren, H.X. Li, M. Dai, D.X. Li, Y. Zhang, J.P. Lang. *Inorg. Chem. Commun.*, **12**, 1168 (2009).
[35] D.S. Deng, L.L. Liu, B.M. Ji, G.J. Yin, C.X. Du. *Cryst. Growth Des.*, **12**, 5338 (2012).
[36] X. Liu, G.C. Guo, A.Q. Wu, L.Z. Cai, J.S. Huang. *Inorg. Chem.*, **44**, 4282 (2005).
[37] (a) Z. Sun, L.M. Fan, W. Zhang, D.C. Li, P.H. Wei, B. Li, G.Z. Liu, L.J. Tian, X.T. Zhang. *J. Coord. Chem*., **65**, 1847 (2012); (b) L.L. Wu, H.H. Song. *J. Coord. Chem*., **65**, 2135 (2012); (c) H.X. Guo, Y.C. Ke, J.P. Wang, J. Wu, Z.S. Zheng. *J. Coord. Chem*., **65**, 2365 (2012); (d) L. Yan, W. Liu, C.B. Li, Y.F. Wang. *J. Coord. Chem*., **66**, 995 (2013).
[38] X.L. Wang, C. Qin, E.B. Wang, Z.M. Su. *Chem. –A. Eur. J*., **12**, 2680 (2006).